Surface Science 656 (2017) 60–65

Contents lists available at ScienceDirect

Surface Science

journal homepage: www.elsevier.com/locate/susc

Pd segregation to the surface of Au on Pd(111) and on Pd/TiO_2(110)

Ryan Sharpe[a,b,*], Jon Counsell[a], Michael Bowker[a,c]

[a] Cardiff Catalysis Institute, School of Chemistry, Cardiff University, Cardiff CF10 3AT, UK
[b] Syncat@Beijing, Synfuels China Technology Co. Ltd., Beijing 101407, China
[c] UK Catalysis Hub, Research Campus at Harwell (RCaH), Rutherford Appleton Laboratory, Harwell, Oxon OX11 0FA, UK

ARTICLE INFO

Keywords:
Model catalysts
Nanoparticles
Core-shell
Au-Pd alloys
TiO_2(110)
Pd(111)

ABSTRACT

The interaction of Au and Pd in bimetallic systems is important in a number of areas of technology, especially catalysis. In order to investigate the segregation behaviour in such systems, the interaction of Pd and Au was investigated by surface science methods. In two separate sets of experiments, Au was deposited onto a Pd(111) single crystal, and Pd and Au were sequentially deposited onto TiO_2(110), all in ultra-high vacuum using metal vapour deposition. Heating Au on Pd/TiO_2(110) to 773 K resulted in the loss of the Au signal in the LEIS, whilst still remaining present in the XPS, due to segregation of Pd to the surface and the formation of a Au-Pd core-shell structure. It is likely that this is due to alloying of Au with the Pd and surface dominance of that alloy by Pd. The Au:Pd XPS peak area ratio is found to substantially decrease on annealing Au/Pd(111) above 773 K, corresponding with a large increase in the CO sticking probability to that for clean Pd(111). This further indicates that Au diffuses into the bulk of Pd on annealing to temperatures above 773 K. It therefore appears that Au prefers to be in the bulk in these systems, reflecting the exothermicity of alloy formation.

1. Introduction

Alloyed/bi-metallic catalysts have applications in a wide range of processes, due to their increased activity, stability and selectivity compared to their component metals [1]. The activity of a bimetallic catalyst depends on several factors, including the distribution of electron density over the particle, the positions of the component species on the catalyst and changes in geometry caused by the interactions of the two metals [2].

Au-Pd catalysts are used in a number of applications. There has recently been a large amount of interest in their use in the synthesis of hydrogen peroxide from H_2 and O_2 [3]. Hutchings investigated the synthesis of hydrogen peroxide by the oxidation of hydrogen [4]. Supported Au was found to be very selective when anchored to the right support; however, adding Pd leads to a huge improvement in catalytic activity. Au-Pd bimetallic catalysts are also used for the industrial production of vinyl acetate monomer via the acetoxylation of ethylene [5–7]. The addition of Au to Pd significantly enhances its selectivity, activity and stability [8]. The details of this promotional effect are not completely understood, but it is thought that the role of the gold is to isolate single Pd sites that facilitate the coupling of the necessary surface species to give the desired reaction, whilst inhibiting the formation of undesirable by-products (CO, CO_2 and surface carbon) [9]. Further work has been carried out by Tysoe et al. on the role of Au in this reaction [10], finding that the rate-determining step of the reaction is dependent on the coverage of Au on a Pd(111) surface. Reaction-kinetics measurements showed this increase in reaction rate on the alloy compared to clean Pd(111) was due to an increase in the overall heat of reaction, which lead to the destabilisation of the reactants whilst at the same time stabilising the desired products [11]. Au-Pd alloys have also been shown to have good activity for the hydrodesulphurisation of thiophene [12]. This was thought to be due to the formation of Au_xPd_y clusters which inhibited the formation of palladium sulphide.

Bimetallic catalysts have been found to restructure under reaction conditions [13]. XPS studies by Hutchings et al. found that AuPd bimetallic catalysts supported on a range of oxides were rich in Pd at the surface after H_2O_2 reactivity testing [4]. This was also observed by Catlow et al., who used XAFS/DRIFTS to observed a Pd shell and a Au-rich core following CO-oxidation [14]. Goodman et al. carried out a series of studies of CO oxidation on Au/Pd(100) single crystal model catalysts, finding that higher pressures of CO induced greater segregation of Pd to the surface [15–17] due to the stronger binding energy of CO to Pd than to Au. This was also shown by a DFT study by Guesmi and Zhu, finding that Pd will enrich the surface of an Au-Pd nanocluster in the presence of CO [18,19]. Conversely, Au has been found to enrich the surface under ideal UHV conditions as segregation of Au to the surface of a Pd-Au bimetallic particle has been found to be

* Corresponding author at: Syncat@Beijing, Synfuels China Technology Co. Ltd., Beijing 101407, China.
E-mail address: ryansharpe@synfuelschina.com.cn (R. Sharpe).

http://dx.doi.org/10.1016/j.susc.2016.10.005
Received 23 May 2016; Received in revised form 28 September 2016; Accepted 15 October 2016
Available online 21 October 2016
0039-6028/

thermodynamically favourable [20].

In this paper, we have investigated the interactions between Au and Pd under ultra-high vacuum conditions using x-ray photoelectron spectroscopy (XPS), low energy ion scattering (LEIS) spectroscopy and molecular beam studies. The top layer sensitivity of LEIS combined with the information regarding the chemical state of the surface that XPS provides allows us to follow the formation of the reported core-shell structures.

2. Experimental

The Pd(111) single crystal work was carried out in a home-built UHV stainless-steel chamber capable of performing XPS and molecular beam experiments. The system comprises of a main stainless-steel chamber separated from a side chamber by a gate valve. The pressure in the chamber is kept constant in the order of 10^{-10} mbar by a combination of a turbomolecular pump, rotary pump and a titanium sublimation pump. The sticking measurements were determined using a mass spectrometer to determine the difference in mass 28 signal between a 100% reflected CO beam and that when the beam hits the single crystal sample [21]. This signal is then followed as the surface becomes saturated with CO at which point the signal returns to that for a 100% reflected beam. Effectively the crystal acts as a pump for CO if the sticking probability is significant. The molecular beam system and methodology have been described in detail elsewhere [21].

The Pd(111) crystal was cleaned by flashing to 1200 K, sputtering with Ar^+ at 700 K, flashing again to 1200 K and finally annealing in O_2 whilst the sample cooled to 800 K. This temperature was maintained until all O_2 had been pumped away, upon which a final flashing to 1200 K was carried out.

The palladium sample used was a Pd(111) single crystal. The sample was mounted on and heated resistively by two tungsten wires which passed through grooves in the edges of the crystals. The temperature was measured using a chromel-alumel thermocouple which was attached directly to the sample via a small hole drilled in the side.

Carbon monoxide (Argo Ltd, 99.5%) was dosed on to the Pd(111) sample for the molecular beam experiments.

The TiO_2(110) experiments were performed in a UHV system built by Omicron Vacuum Physik that has been described in detail elsewhere [22]. It is capable of performing X-ray photoelectron spectroscopy (XPS), low energy ion scattering (LEIS/ISS) and low energy electron diffraction (LEED). The system comprises three separate chambers pumped by a combination of four turbomolecular pumps, three titanium sublimation pumps and two ion pumps, resulting in a base pressure of $< 1\times10^{-9}$ mbar.

The TiO_2 sample was cleaned by Ar^+ bombardment at 1 keV, followed by annealing in UHV, typically at 773 K. Surface cleanliness was monitored by XPS and LEIS, and gas purity was analysed using a quadrupole mass spectrometer. XPS spectra were recorded at room temperature (~300 K) using an Al Kα photon source, a detection angle of 90° and an analyser pass energy of 50 eV unless stated otherwise. All XPS data was analysed with CasaXPS [23] and binding energies were calibrated to the O(1 s) peak at 530.4 eV [24]. LEIS spectra were recorded at room temperature using helium gas, a primary energy of 1000 eV and a scattering angle of 135°.

The titanium dioxide sample used was a TiO_2(110) single crystal (Pi-Kem Ltd). The sample was mounted on a standard Omicron molybdenum plate via spot-welded Ta strips. A thermocouple was attached to the sample plate holder for temperature measurement.

Palladium and gold were deposited at room temperature via metal vapour deposition (MVD). The source of Pd was a Pd wire (0.125 mm, Goodfellow, 99.95%) tightly wrapped around a W filament (0.25 mm, Advent, 99.95%). The source of Au was a Au bead (from foil, Goodfellow, 99.99%) formed on a W coil. These were resistively heated by passing a current of 3 A through the coil in UHV.

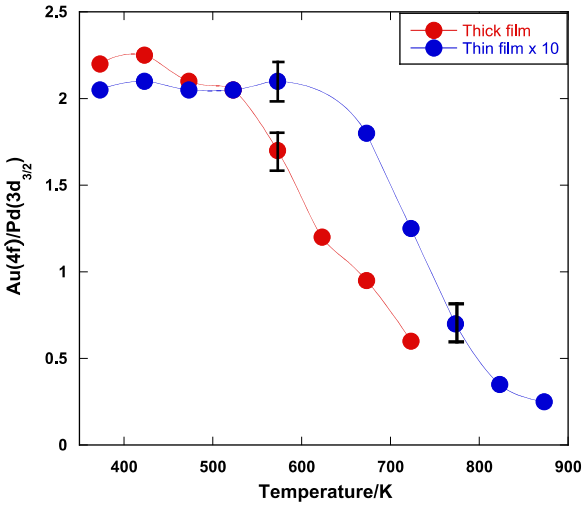

Fig. 1. Au4f/Pd3d XPS peak area ratio vs annealing temperature for thick and thin films of Au on Pd(111).

3. Results

3.1. Au on Pd(111) single crystals

Two different amounts of Au were dosed onto the Pd(111) surface (7.5 ± 1.0 and 1.3 ± 0.4 ML, taking 400 s and 50 s dosing time respectively) and the sample was heated to increasing temperatures for 5 min at a time. Molecular beam experiments were carried out at room temperature.

Fig. 1 shows the effect of annealing on the Au/Pd XPS peak area ratio for the thick film of Au/Pd(111) and for the thin film of Au/Pd(111). The ratio for the thick Au film gradually decreases up to 548 K, and then decreases more significantly at higher temperatures. This result is broadly similar to the thin Au film, with constant ratio at low temperature followed by a massive decrease at high temperature. The main difference, however, is that the transition temperature is somewhat higher than for the higher coverage, occurring at ~ 600 K vs 550 K for the higher gold coverage.

CO sticking was also measured out on the thin film of Au on the Pd(111) crystal, the results of which are shown in Fig. 2. Au was deposited for 50 s at room temperature and the surface was then annealed at increasing temperatures for 5 min at a time. After each heating cycle, the sample was cooled to 393 K after which CO was introduced to the surface in the beam. As the sample was heated to

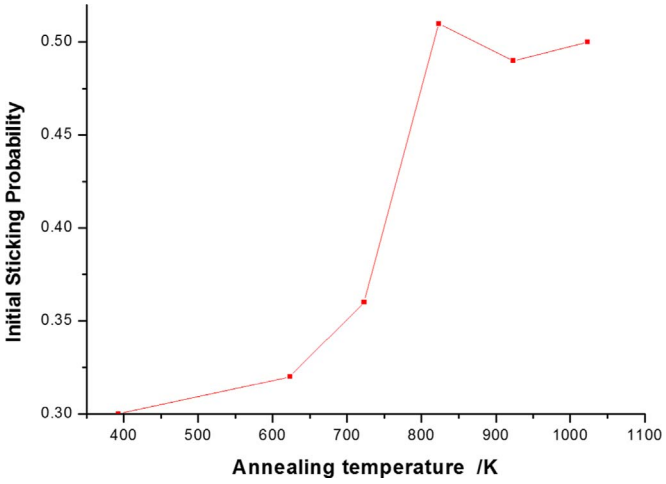

Fig. 2. Initial sticking probability of CO at 393 K after annealing a Au dosed (50 s) Pd (111) surface at increasing temperatures for 300 s.

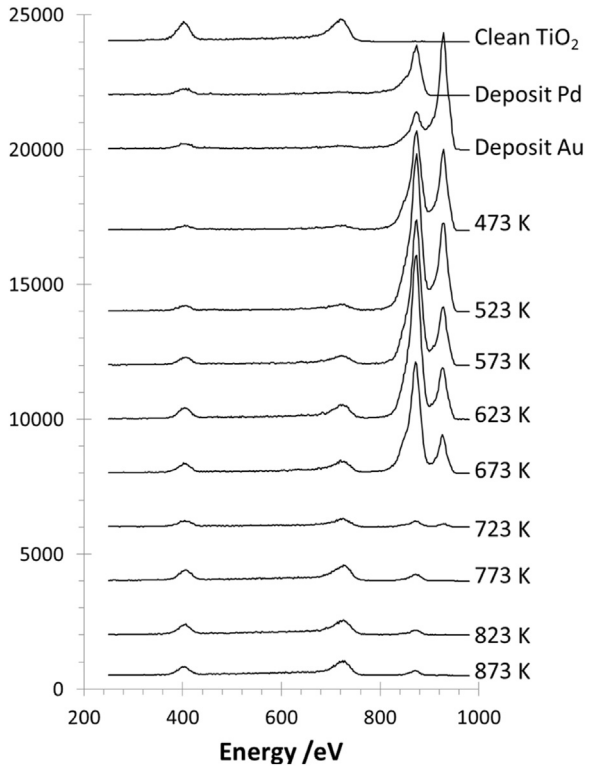

Fig. 3. LEIS spectra showing the sequential deposition of Pd and Au on the TiO_2(110) surface and subsequent annealing at increasing incremental temperatures.

higher temperatures, the initial sticking probability of CO increased significantly to that reported for Pd(111) [25,26]. However, clearly the sticking probability was not zero, as it might be expected to be for Au, and as it was for the thick film. Thus it appears that some Pd sites were still available for the thin film, and saturation of the CO adsorption was at 1/3 of that for the clean Pd surface.

3.2. Au and Pd on TiO_2(110) single crystals

The TiO_2(110) surface was cleaned via repeated sputtering and annealing cycles, as described in the experimental section above. Pd and Au were sequentially deposited on to the clean surface, which was then annealed at increasing temperatures in increments, from 473 K to 873 K. The resulting LEIS data is shown in Fig. 3. On clean titania, the O signal can be seen at ~410 eV and the Ti signal can be seen at ~740 eV. After deposition of Pd for 150 s, giving a film of ~1.3 nm (~5 ML, based on a (111) type film as reported earlier [27]), the Ti signal is almost completely absent from the spectra, whilst the oxygen signal has substantially decreased. The Pd signal can be seen at ~880 eV. Au is then deposited for 80 s, giving a film of ~0.1 nm – the resulting peak can be seen at ~930 eV, and the Pd peak is diminished. On annealing at 473 K for 10 min, the Au signal immediately decreases, whilst the Pd signal increases. At the same time, the Ti signal has re-emerged. Fig. 4 shows that the Au:Pd LEIS ratio decreases by a factor of ~3.7. On annealing to higher temperatures the Ti signal continues to increase, whereas the Au signal decreases further, until it completely disappears from the spectrum at 773 K. At temperatures above 773 K, the Pd signal decreases further, the Ti and O signals increase, and Au does not reappear in the spectra. Fig. 5 shows the XPS area ratios – the Au4f:Pd3d ratios do not change drastically on annealing, although they do tend to decrease.

The raw XPS data are shown in Fig. 6 and are described as follows; the Ti2p XPS (Fig. 6a) shows a decrease in signal on deposition of the metals and an increase in signal after annealing. The $2p_{3/2}$ peak can be seen at 459 eV and the $Ti2p_{1/2}$ peak is at 464 eV. The Pd3d and Au4f

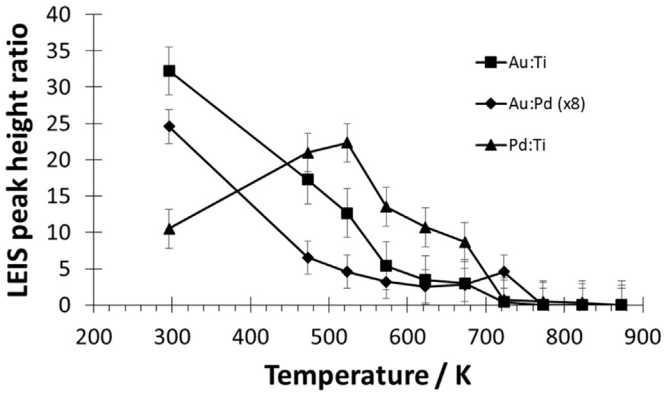

Fig. 4. LEIS peak height ratios taken from Fig. 3.

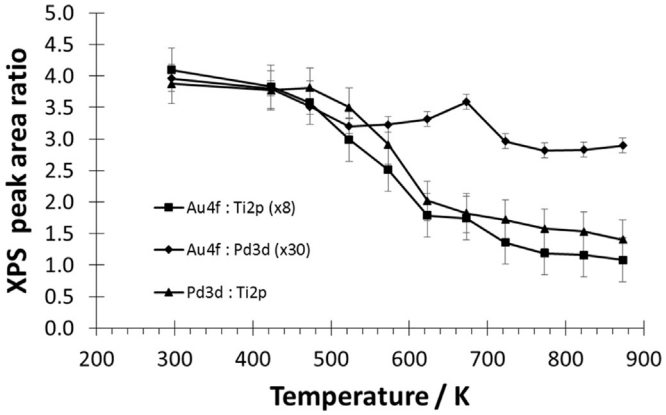

Fig. 5. XPS peak area ratios taken from Fig. 6.

spectra (Fig. 6b and c, respectively) show that the metal signals decrease on annealing. In the Pd3d spectra, the peak at 335 eV is the $Pd3d_{5/2}$, and the peak at 340 eV is $Pd3d_{3/2}$. The peak at 84 eV in the Au4f spectra is the 4 $f_{7/2}$ peak, and the peak at 88 eV is the 4 $f_{5/2}$ peak. Note that the $Au4f_{7/2}$ peak should be 4/3 times bigger than the 4 $f_{5/2}$ peak due to spin orbit splitting, however, the 4 $f_{5/2}$ peak is approximately the same size as the 4 $f_{7/2}$ peak, due to the contribution of the Pd1s peak which occurs at 88 eV. Fig. 7 shows the C1s spectra before and after depositing Pd on to clean TiO_2(110). A small carbon signal can clearly be seen at ~285 eV after the Pd is deposited.

4. Discussion

4.1. Au on Pd(111) single crystals

The experiments on this system were made in order to understand the behaviour of segregation in the unsupported pure metals system, and to gain insight into the nature of the surface layers upon annealing. Increased CO adsorption after annealing to higher temperatures shown in Fig. 2 can be attributed to loss of surface Au to the bulk of the sample. This agrees with the XPS data shown in Fig. 1, which shows a decreasing Au/Pd XPS peak area ratio on annealing. The Au/Pd ratio in Fig. 1 at 400 K is 0.21 which corresponds to a surface coverage of around 2/3 of a monolayer of Au and a CO sticking probability of 0.3. When the sample is annealed to 723 K, the Au/Pd ratio drops to 0.12, which corresponds to a higher CO sticking probability of ~0.37. When the Au/Pd ratio is at its lowest, on annealing to 823 K, the CO sticking probability increases to ~0.51. This value is the same as that found in the same system for the clean Pd(111) surface [26]. These results agree with a LEIS study by Tysoe et al. on Au/Pd(111), which found that the Au coverage on the outermost layer started to decrease on annealing to 600 K and then decreased substantially at 700 K [28]. Tysoe et al.

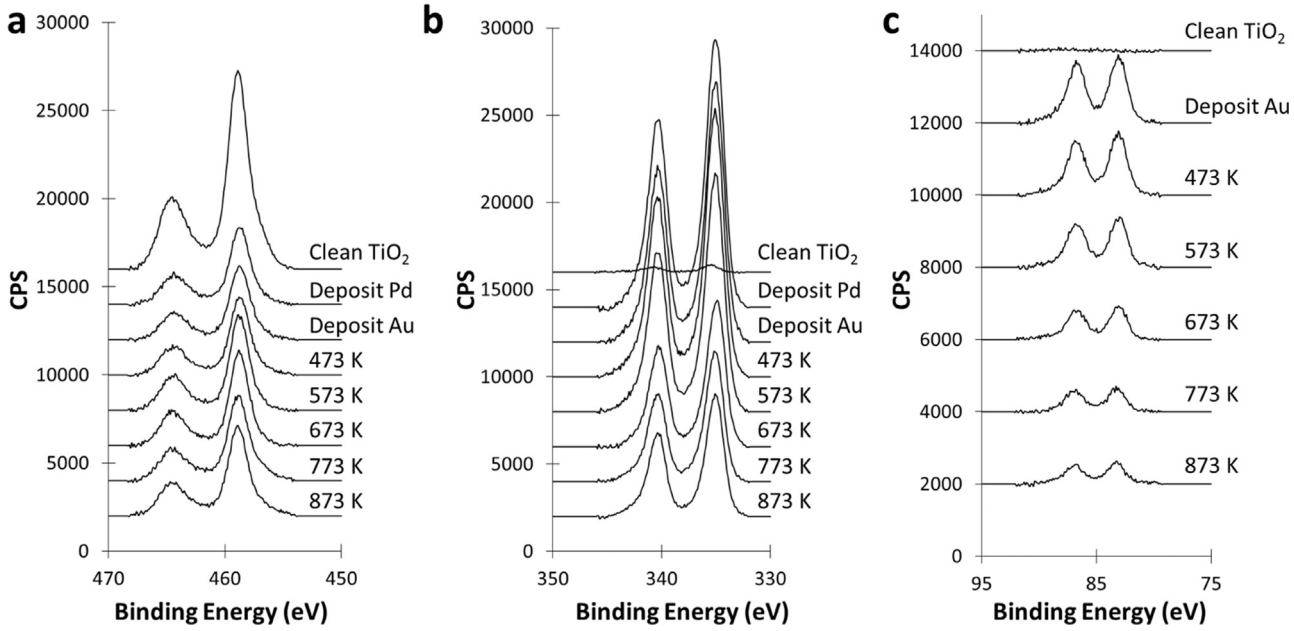

Fig. 6. XPS raw data shown for a) Ti2p, b) Pd3d and c) Au4f, taken after depositing Pd and Au on to TiO_2(110) and then annealing at increasing incremental temperatures.

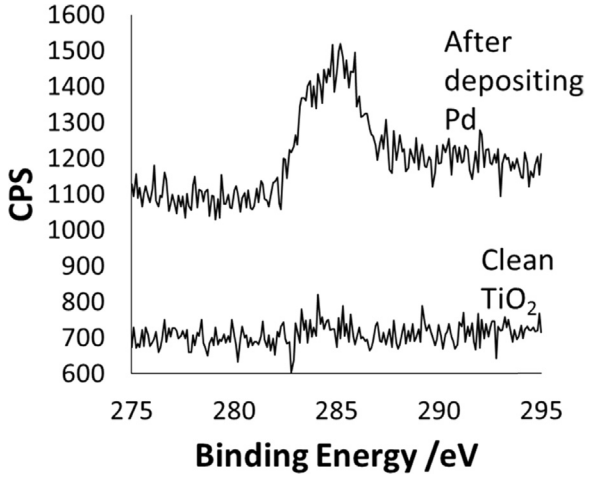

Fig. 7. C1s XPS raw data taken before and after depositing Pd on to clean TiO_2(110).

found further evidence for this using CO TPD and RAIRS study on both Au/Pd(111) [29] and Au/Pd(100) [30]. LEED results showed, however, that the second-layer gold coverage was always lower than that in the outermost layer [28]. Auger electron spectroscopy studies carried out by Baddeley et al. on Au/Pd(111) describe similar results, finding that annealing results in the formation of random surface AuPd alloys with increasing Pd content at higher temperatures [31]. This differs somewhat from a LEIS and STM study by Goodman and coworkers, who demonstrated the preferential segregation of Au on Au/Pd(100) after sputtering and annealing, and showed that annealing Au_3Pd(100) in UHV resulted in a pure outermost layer of Au [32]. The difference between Goodman's results and the results presented in this paper are possibly due to the different quantities of Au deposited. In our experiments, the equilibrium bulk Au concentration is close to zero, which results in a low equilibrium surface concentration.

4.2. Au and Pd on TiO_2(110) single crystals

The disappearance of the Au signal from the LEIS after annealing suggests several possibilities; the Au may have evaporated from the surface, or there may be no Au in the surface layers, or considerable sintering has occurred to leave the vast majority of the surface clean. However, the Au signal is still very much present in the XPS after annealing (see Fig. 4c), so it has obviously not left the surface or left a large majority uncovered. This agrees with previous work that shows that Au desorption has an onset temperature of ~1000 K on TiO_2(110) [33]. Taking this into account, it seems most likely that, upon heating, the Au and Pd form bimetallic particles (as evidenced by the reappearance of the Ti signal in the LEIS and the decline in the metal/Ti ratios between 523 K and 673 K in Figs. 3, 4 and 5), with a Au-core and a Pd-shell. This is surprising as, under ideal conditions, Au/Pd clusters are expected to form Au-shell Pd-core structures [20,34–37] as segregation of Au to the surface of a Pd-Au bimetallic particle has been found to be thermodynamically favourable [20]. The surface free energy for Au is 1.63 J m^{-2}, whereas the corresponding value for Pd is 2.04 J m^{-2} [38], which should favour enrichment of the surface with Au. Pd-core Au-shell particles were found to be the most stable when analysed using classic molecular dynamics simulation [34], and, according to these calculations, can even be formed when annealing other structures, e.g. Au-core Pd-shell particles. However, Au-core Pd-shell structures have been observed when kinetics dominate over thermodynamic factors [39–41] or when the Pd has been oxidised [42]. Davies et al. observed the formation of Au-core Pd-shell nanoparticles on γ-Fe_2O_3 [2]. They found that the Au signal disappeared from the LEIS after annealing to 573 K, and observed particles with STM. The formation of these particles was attributed to the oxidation of the Pd, however they could not be conclusive about this due to the lack of XPS or similar surface-sensitive technique. This is unlikely to be a factor in our case, however, as the Pd 3d XPS shows no signs of oxidation – PdO appears at 336–336.4 eV whereas the Pd metal signal appears at 335.1 eV [43]. However, the LEIS spectra do show an oxygen signal even when the Ti signal is lost as it is covered by the Pd (Fig. 3). Furthermore, there is a carbon signal present in the C1s XPS on deposition of the Pd (Fig. 7). It is possible that the Pd has adsorbed CO from the chamber; CO has a very high sticking probability on Pd [44,45], as described above, which will affect the surface free energy of the Pd once it is adsorbed. Guesmi and Zhu carried out a combined DFT and DRIFTS study, finding that Pd will enrich the surface of an Au-Pd nanocluster in the presence of CO [18]. The question of why C is not observed in the LEIS whereas Pd is observed is answered by Shen et al., who adsorbed CO onto Cu_3Pt(111) and found only O, Cu and Pt peaks in the LEIS [46], indicating that the orientation of the CO molecule was with the O facing

away from the surface. Presumably this is also the case here with Pd/TiO_2(110) – the CO binds via the C (hence C is not seen in the LEIS) and there is not full coverage of CO on the Pd (therefore Pd is still seen in LEIS spectra). However, it's likely that the presence of CO has a negligible effect in our case, as our experiments were carried out under UHV conditions (typically $< 1\times10^{-9}$ mbar). Goodman et al. examined the effect of CO on AuPd(100) alloys at low pressures of CO and found that a pressure of 10^{-5} mbar was required to achieve a notable, but still small effect [16]. A pressure of 10^{-7} CO was also investigated, with no notable surface segregation of the Pd.

It's interesting to note that Davies et al. [2] saw the Au signal disappear from the LEIS at 573 K, whereas the Au signal in Fig. 3 does not disappear until 773 K. This may be due to the amounts of Pd and Au deposited onto each surface. Davies evaporated only 10 s of Pd and Au onto the Fe_2O_3 surface forming only small nanoparticles between 5 and 10 nm in size, whereas we have evaporated a thin film onto the TiO_2 surface. A study by Freund found the opposite occurrence – after co-depositing Pd and Au onto various well-ordered oxide films [e.g. MgO(100), CeO_2(111), Fe_3O_4(111)] and annealing to 600 K with alternating O_2 and CO treatments, Au was found to segregate to the surface. Au surface enrichment on annealing has also been described by several other authors – Goodman et al. used LEIS, XPS and carbon monoxide TPD to show that annealing a Pd-Au mixture on Mo(110) at 800 K leads to a surface alloy that is 80% Au. The formation of unexpected core-shell structures has also been found with other elements - a combined XPS and LEIS study of Pt & Au on TiO_2(110) was carried out by Chen et al. [33]. LEIS showed that deposition of Au on Pt did not result in core-shell structures with Au on top, as predicted for the bulk phase. Instead, the clusters were 10–30% richer in Pt at the surface compared to the overall composition.

It is notable that, on annealing to 473 K and 523 K, the Pd signal in the LEIS is larger than when it was first deposited. This is presumably due to a combination of desorption of background gases, especially CO, and the inward diffusion of Au. Ovari et al. observed a similar increase in Au LEIS signal on deposition of Rh on Au-TiO_2(110) at room temperature, suggesting that the enhancement of the Au LEIS peak was because the Rh atoms moved to subsurface sites [47]. The enhanced volume of the bimetallic clusters with the Au atoms outside led to the increase in LEIS intensity.

At 723 K there is a dramatic drop in the Pd and Au LEIS signals, whilst the Pd 3d and Au 4f XPS peaks are still large. At the same time, the Ti 2p peaks have not recovered their initial intensities at this temperature. This suggests that some encapsulation of the particles may have taken place, known as the SMSI (strong metal-support interaction) effect. However, the onset of encapsulation by TiOx (where x ~ 1 [47]) is typically accompanied by the emergence of a shoulder peak in the Ti 2p spectrum at 455.5 eV, characteristic of Ti^{2+} [22], whereas we do not see the appearance of any Ti^{2+} or Ti^{3+} in the XPS (Fig. 6a). However, this is probably because the amount of TiO_x in this layer is very small compared with that from the support crystal, masking that signal. Indeed, in our earlier work [47], it was only at grazing exit that we could clearly identify the Ti^{2+} state.

There has been a large amount of work looking at the SMSI effect on Pd and Au separately, finding that Pd is easily encapsulated by titania on annealing whereas Au is not [22]. This encapsulation layer has been found to be a TiO or $TiO_{1.4}$ overlayer [27,48] and has also been observed on other systems, including Pt/TiO_2 [49–52] and Rh/TiO_2 [53]. Although, to the best of our knowledge, there are no studies examining the SMSI effect on Au-Pd systems, there is some work examining the Au-Pt and Au-Rh systems on TiO_2(110). In particular, Ovari et al. have looked extensively at Au-Rh thin films and nanoparticles on TiO_2(110) [47,54–56], finding that, whilst monometallic Rh clusters on TiO_2(110) are encapsulated at ~750 K by the oxide, encapsulation is negligible for the bimetallic Rh-Au particles almost completely covered by Au [47]. This group also looked at the deposition of Au on Rh nanoparticles that had undergone SMSI and were encapsulated by a thin film of TiOx. On annealing to 900 K, this TiOx layer had been replaced by a Au ultrathin layer [56]. Similar results have been found with Au-Pt/TiO_2(110). Grazing angle XPS by Park et al. showed that annealing Au-Pt clusters on TiO_2 (110) to temperatures greater than 600 K induced encapsulation of the clusters, but the presence of Au at the cluster surface decreased the extent of encapsulation compared to pure Pt clusters [33]. This was further shown with LEIS, where they were able to observe uncovered Pt sites up to 1000 K [33]. This agreed with experiments later carried out by Tenney et al., finding that annealing Pt clusters on titania causes the reduction of the support as the clusters become encapsulated by TiOx, whilst reduction of the titania does not occur when Pt clusters are covered by Au [57,58]. This is somewhat contrary to what we see in the LEIS (Fig. 3) on annealing to 773 K, where the Au has disappeared from the spectra whilst the Pd still remains visible. It is possible the formation of a Pd-Ti alloy is a driver for enabling the SMSI effect to occur, as has been reported for TiOx films grown on Pt surfaces [59] and on Pd(111) and (100) surfaces [60].

The Au4f:Pd3d XPS ratios shown in Fig. 5 do not change drastically on annealing, suggesting that the Pd shell around the Au cannot be thicker than a few nanometres – if it was thicker, the Au signal would decrease relative to the Pd signal on annealing to higher temperatures, as the XPS would be unable to penetrate the Pd layer. This suggests that the AuPd has formed a structure with a Pd shell and an alloyed Au/Pd core. Wells et al. propose a similar structure based on EXAFS results – they propose a gold rich core and a AuPd alloy layer, with a skin of Pd at the surface following CO oxidation conditions [14]. We note that Wilson et al. made Pd@Au nanoparticles (~15 nm in diameter) supported on SiO_2 [61]. They found that Pd remains at the surface after heating to 100 °C, and even after reduction at 300 °C, that the surface was still dominated by Pd-CO bands in IR, though some alloying had occurred. In this case the total Pd:Au ratio was low, at a maximum of ~0.3.

5. Conclusions

Using a combination of XPS and LEIS we have fabricated Pd-Au bimetallic structures on TiO_2(110) under ultra-high vacuum. Au was deposited onto Pd on TiO_2(110) but, after annealing to 773 K, Pd segregated to the surface to form an Pd-shell Au-core structure, the core being an alloy with Pd. At the same time, the encapsulation of the Pd-Au particles by TiOx was observed. The diffusion of Au into the bulk of Pd has also been observed on a Pd(111) single crystal by an increase in CO sticking probability to the clean Pd(111) surface value after annealing to 800 K, and by a decrease in Au/Pd XPS peak area ratio on annealing to temperatures above 700 K.

Further information

Information concerning the data supporting the research results presented here, including how to assess that data, can be found in the Cardiff University data catalogue at http://dx.doi.org/10.17035/d.2016.0009299603.

Acknowledgements

We are grateful to Cardiff University for studentships to RS and JC, and to part funding of RS from EPSRC via an institutional DTA grant. RS thanks Dr Rob Davies of Imperial College London and Dr Dave Morgan of Cardiff University for their technical assistance.

References

[1] V. Ponec, Appl. Catal. a-Gen. 222 (2001) 31.
[2] R.J. Davies, M. Bowker, P.R. Davies, D.J. Morgan, Nanoscale 5 (2013) 9018.
[3] S.J. Freakley, M. Piccinini, J.K. Edwards, E.N. Ntainjua, J.A. Moulijn,

G.J. Hutchings, ACS Catal. 3 (2013) 487.
[4] P. Landon, P.J. Collier, A.F. Carley, D. Chadwick, A.J. Papworth, A. Burrows, C.J. Kiely, G.J. Hutchings, Phys. Chem. Chem. Phys. 5 (2003) 1917.
[5] M.H. Zhang, M.X. Gao, Q. Li, M.L. Tao, Y.Z. Yu, RSC Adv. 4 (2014) 17709.
[6] M.S. Chen, D.W. Goodman, Chin. J. Catal. 29 (2008) 1178.
[7] M.S. Chen, D. Kumar, C.W. Yi, D.W. Goodman, Science 310 (2005) 291.
[8] D. Kumar, M.S. Chen, D.W. Goodman, Catal. Today 123 (2007) 77.
[9] X.W. Liu, D.S. Wang, Y.D. Li, Nano Today 7 (2012) 448.
[10] F. Calaza, M. Mahapatra, M. Neurock, W.T. Tysoe, J. Catal. 312 (2014) 37.
[11] F. Calaza, Z.J. Li, M. Garvey, M. Neurock, W.T. Tysoe, Catal. Lett 143 (2013) 756.
[12] A.M. Venezia, V. La Parola, V. Nicoli, G. Deganello, J. Catal. 212 (2002) 56.
[13] F. Tao, M.E. Grass, Y.W. Zhang, D.R. Butcher, J.R. Renzas, Z. Liu, J.Y. Chung, B.S. Mun, M. Salmeron, G.A. Somorjai, Science 322 (2008) 932.
[14] E.K. Gibson, A.M. Beale, C.R.A. Catlow, A. Chutia, D. Gianolio, A. Gould, A. Kroner, K.M.H. Mohammed, M. Perdjon, S.M. Rogers, P.P. Wells, Chem. Mater. 27 (2015) 3714.
[15] F. Gao, Y.L. Wang, D.W. Goodman, J. Catal. 268 (2009) 115.
[16] F. Gao, Y.L. Wang, D.W. Goodman, J. Phys. Chem. C 113 (2009) 14993.
[17] F. Gao, Y.L. Wang, D.W. Goodman, J. Am. Chem. Soc. 131 (2009) 5734.
[18] B. Zhu, G. Thrimurthulu, L. Delannoy, C. Louis, C. Mottet, J. Creuze, B. Legrand, H. Guesmi, J. Catal. 308 (2013) 272.
[19] M. Sansa, A. Dhouib, H. Guesmi, J. Chem. Phys. (2014) 141.
[20] I.V. Yudanov, K.M. Neyman, Phys. Chem. Chem. Phys. 12 (2010) 5094.
[21] M. Bowker, R. Holroyd, N. Perkins, J. Bhantoo, J. Counsell, A. Carley, C. Morgan, Surf. Sci. 601 (2007) 3651.
[22] M. Bowker, R. Sharpe, Catal. Struct. React. 1 (2015) 140.
[23] N. Fairley, CasaXPS, Version 2.3.15, Casa Software Ltd, 1999-2011.
[24] U. Diebold, T. Madey, Surf. Sci. Spectra 4 (1997) 227.
[25] T. Engel, J.Chem. Phys. 69 (1978) 373.
[26] J. Counsell, ⟨http://orca.cf.ac.uk/54930/⟩, 2010, [Ph.D. thesis].
[27] R.A. Bennett, C.L. Pang, N. Perkins, R.D. Smith, P. Morrall, R.I. Kvon, M. Bowker, J. Phys. Chem. B 106 (2002) 4688.
[28] Z.J. Li, O. Furlong, F. Calaza, L. Burkholder, H.C. Poon, D. Saldin, W.T. Tysoe, Surf. Sci. 602 (2008) 1084.
[29] Z.J. Li, F. Gao, Y.L. Wang, F. Calaza, L. Burkholder, W.T. Tysoe, Surf. Sci. 601 (2007) 1898.
[30] Z.J. Li, F. Gao, O. Furlong, W.T. Tysoe, Surf. Sci. 604 (2010) 136.
[31] C.J. Baddeley, M. Tikhov, C. Hardacre, J.R. Lomas, R.M. Lambert, J. Phys. Chem. 100 (1996) 2189.
[32] P. Han, S. Axnanda, I. Lyubinetsky, D.W. Goodman, J. Am. Chem. Soc. 129 (2007) 14355.
[33] J.B. Park, S.F. Conner, D.A. Chen, J. Phys. Chem. C 112 (2008) 5490.
[34] H.B. Liu, U. Pal, R. Perez, J.A. Ascencio, J.Phys. Chem. B 110 (2006) 5191.
[35] O.A. Oviedo, L. Reinaudi, M.M. Mariscal, E.P.M. Leiva, Electrochim. Acta 76 (2012) 424.
[36] X. Wu, Y.J. Dong, N. J. Chem. 38 (2014) 4893.
[37] R. Marchal, A. Genest, S. Kruger, N. Rosch, J. Phys. Chem. C 117 (2013) 21810.
[38] M.S. Chen, K. Luo, T. Wei, Z. Yan, D. Kumar, C.W. Yi, D.W. Goodman, Catal. Today 117 (2006) 37.
[39] A.F. Lee, C.J. Baddeley, C. Hardacre, R.M. Ormerod, R.M. Lambert, G. Schmid, H. West, J. Phys. Chem. 99 (1995) 6096.
[40] Y. Kobayashi, S. Kiao, M. Seto, H. Takatani, M. Nakanishi, R. Oshima, Hyperfine Interactions 156 (2004) 75.
[41] Y.W. Lee, M. Kim, Z.H. Kim, S.W. Han, J. Am. Chem. Soc. 131 (2009) 17036.
[42] J.K. Edwards, B.E. Solsona, P. Landon, A.F. Carley, A. Herzing, C.J. Kiely, G.J. Hutchings, J. Catal. 236 (2005) 69.
[43] D. Briggs, M. Seah, Practical Surface Analysis by Auger and X-ray Photoelectron Spectroscopy, John Wiley & Sons, Chichester, 1983.
[44] M. Bowker, I.Z. Jones, R.A. Bennett, S. Poulston, Catal. Autom. Pollut. Control IV 116 (1998) 431.
[45] M. Bowker, P. Stone, R. Bennett, N. Perkins, Surf. Sci. 497 (2002) 155.
[46] Y.G. Shen, D.J. Oconnor, K. Wandelt, R.J. Macdonald, Surf. Sci. 331 (1995) 746.
[47] L. Ovari, L. Bugyi, Z. Majzik, A. Berko, J. Kiss, J. Phys. Chem. C 112 (2008) 18011.
[48] R.A. Bennett, P. Stone, M. Bowker, Catal. Lett. 59 (1999) 99.
[49] F. Pesty, H.P. Steinruck, T.E. Madey, Surf. Sci. 339 (1995) 83.
[50] Y. Gao, Y. Liang, S.A. Chambers, Surf. Sci. 365 (1996) 638.
[51] H.P. Steinruck, F. Pesty, L. Zhang, T.E. Madey, Phys. Rev. B 51 (1995) 2427.
[52] S. Bonanni, K. Ait-Mansour, H. Brune, W. Harbich, ACS Catal. 1 (2011) 385.
[53] A. Berko, I. Ulrych, K.C. Prince, J. Phys. Chem. B 102 (1998) 3379.
[54] L. Ovari, A. Berko, N. Balazs, Z. Majzik, J. Kiss, Langmuir 26 (2010) 2167.
[55] L. Ovari, A. Berko, R. Gubo, A. Racz, Z. Konya, J. Phys. Chem. C 118 (2014) 12340.
[56] R. Gubo, L. Ovari, Z. Konya, A. Berko, Langmuir 30 (2014) 14545.
[57] S.A. Tenney, W. He, J.S. Ratliff, D.R. Mullins, D.A. Chen, Top. Catal. 54 (2011) 42.
[58] S.A. Tenney, J.S. Ratliff, C.C. Roberts, W. He, S.C. Ammal, A. Heyden, D.A. Chen, J. Phys. Chem. C 114 (2010) 21652.
[59] T. Matsumoto, M. Batzill, S. Hsieh, B.E. Koel, Surf. Sci. 572 (2004) 127.
[60] M.H. Farstad, D. Ragazzon, H. Gronbeck, M.D. Stromsheim, C. Stavrakas, J. Gustafson, A. Sandell, A. Borg, Surf. Sci. 649 (2016) 80.
[61] A.R. Wilson, K.Y. Sun, M.F. Chi, R.M. White, J.M. LeBeau, H.H. Lamb, B.J. Wiley, J. Phys. Chem. C 117 (2013) 17557.